Journal of Basic Physical Research ISSN: 2141-8403 Prints, 2141-8411 Online
Vol.11, No.2 pp. 1- 9, Sept., 2023. Available online at www.jbasicphyres-unizik.org

OPTIMIZING SEISMIC DATA ACQUISITION FOR SUBSURFACE EXPLORATION: A CASE STUDY OF NIGER DELTA

Onwubuariri, Chukwuebuka Nnamdi[1,2]*, Anakwuba, Emmanuel Kenechukwu[2], Dinneya, Obinna Christian[1], Nwokoma, Esomchi Uzoma[1].
1(Department of Physics, Michael Okpara University of Agriculture, Umudike, Abia State, Nigeria)
2(Department of Geophysics, Nnamdi Azikiwe University, Awka, Anambra State, Nigeria)
onwubuariri.chukwuebuka@mouau.edu.ng

Abstract
The seismic reflection method has played a crucial role in geological exploration, spanning from petroleum to engineering investigations. This study aims to enhance seismic acquisition in the demanding Niger Delta terrain, particularly in the OML 28 block, considering environmental and urban complexities. A comprehensive 3D reshoot seismic survey was conducted, involving systematic partitioning of the field into 7 swaths, while ensuring quality control measures. Shot points that fell on non-seismic objects were strategically relocated to ensure full-fold coverage and adequate subsurface sampling without having any negative environmental implications, utilizing techniques like point shift, smooth curve and laminar flow. Fold coverage analysis delineated distinct ranges across various offsets, including near, mid, far, and full offsets. Notably, the nominal full-fold coverage for OML 28 was 312, with observable improvements in mid-offset ranges compared to near-offset and far-offset. Merging offset ranges facilitated achieving the required fold through swath overlap, ensuring thorough subsurface sampling. Additional analyses encompassed bin statistics, offset/azimuth rose diagrams, and surface topography examination, shedding light on trace distribution and elevation variations. Drilling operations were essential, revealing disparities between drilled and loaded depths, indicating potential signal attenuation concerns. Arrival time analysis emphasized drilling past weathered layers to mitigate signal attenuation. This study enhances seismic acquisition optimization, providing insights into fold coverage variations across offsets and emphasizing comprehensive drilling practices for signal enhancement. These findings are crucial for refining subsurface imaging and geological comprehension, particularly in challenging terrains like the Niger Delta.
Keywords: *Seismic acquisition, GBARAN field, Fold coverage, Weathered layers, Offset ranges*

Introduction

The seismic approach has historically proven effective in identifying various geological features, including salt domes, oil wells, and ore minerals (Bridle et. al., 2009; Ajani et. al., 2013). This technique has witnessed significant advancements since the 1960s, with the introduction of common depth point (CDP) surveying and magnetic tape recording (Zanzi *et al*., 1991). The seismic reflection method, essential for petroleum exploration, has evolved into a sophisticated geophysical tool. Current research focuses on 4-D and 4-C technologies, emphasising computer technology applications for time-lapse 3-D methodologies and the use of three-component geophones for shear wave identification (Opara et. al., 2018; Opara et. al., 2017; Adizua et. al., 2019).

Beyond petroleum exploration, seismic acquisition finds utility in engineering site investigations, hydrogeological research, shallow stratigraphy, and archaeology. Shallow subsurface investigations, defined as operations conducted at depths less than 100 metres, have adapted technology from petroleum exploration. Limited resources often lead to a superficial approach in these investigations (Yordkayhun et. al., 2007; Hewitt, 1980; Onwubuariri et. al., 2023).

The efficacy of seismic acquisition in deep subsurface areas, exemplified in the OML 28 block case study, encounters challenges in urban areas with dense populations. Environmental variables, noise interference, and non-seismic objects can compromise the integrity of data. To address these challenges, there is a need for a model optimising the process to avoid environmentally damaging energy sources like explosives commonly used in the Niger Delta. The study emphasises determining target depth, velocity of consolidated layers, and weathered layer thickness during 3D acquisition and subsequent 4D acquisition. Uphole or downhole surveys play a crucial role in determining weathered layer thickness and seismic velocities in the weathered zone before 3D reflection acquisition (Kolawole et. al., 2012; Cordsen et. al., 2000). The study aims to identify the optimal burial depth for explosives, considering the thickness of the weathered layer and the unconsolidated layer.

Location, Terrain and geology of the study area

The 3D reshoot seismic survey was conducted in the Gbaran (OML 28) block, spanning Easting 447,270 to 422,070 longitude and Northing 131,350 to 105910 latitude. Located in the south-south region of Nigeria's Niger Delta, the study site encompasses 571.15 square kilometres between Bayelsa and Rivers States, with notable rural-urban areas. The region comprises six primary local government areas: Ahoada West, Abua/Odua, Kolokuma/Opokuma, Sagbama, Yenagoa, and Ogbia, cultivating cassava and cash crops in the rural sectors.

The terrain exhibits sandy, marshy, and muddy conditions with undulating topography, lacking distinct boundaries between elevated and lower areas. The presence of dense vegetation, particularly in the north-western region, has led to logging activities, impacting data quality. The vegetation makeup consists of approximately 60% upland rainforest in the southeastern and northeastern sectors, while 40% comprises swampy raffia palm and floating grass along the inclined channels of the Orashi River and Nun River to the southwest.

The geological context of the Niger Delta Basin reveals its formation through a failed rift junction during the separation of the South American and African plates, leading to the South Atlantic Ocean. Late Jurassic to mid-Cretaceous rifting occurred, creating thrust faults, and syn-rift sands and shales were deposited (Anomoharan, 2014; Kolawole et. al., 2012). The ongoing rifting process, high-angle normal faults, and fault block rotation characterised the late Cretaceous period. The Akata Formation and Agbada Formation were produced during the Paleocene and Eocene, respectively. The Oligocene saw the deposition of the Benin Formation. The basin's geological complexity is evident in its diverse zones, from the continental shelf's extensional zone to the deep-sea contraction zone. (Ejedawe, 1981; Doust & Omatsola, 1990) The sedimentary deposits in the Niger Delta exhibit variations in lithologies influenced by factors such as sea level, volcanic activity, tides, and sequence stratigraphy. Figures 1 and 2 illustrate the map of the Niger Delta and the study location.

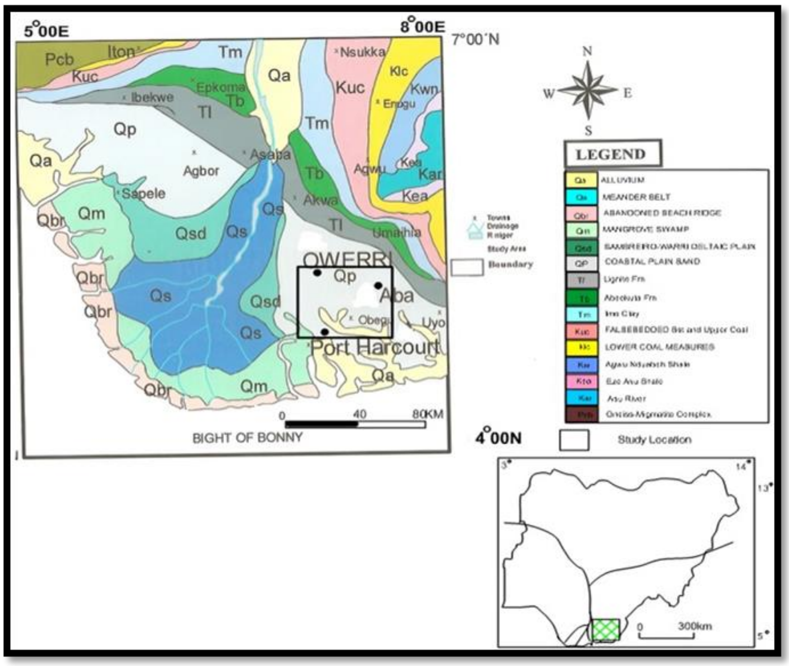

Figure 1: Map of Niger delta

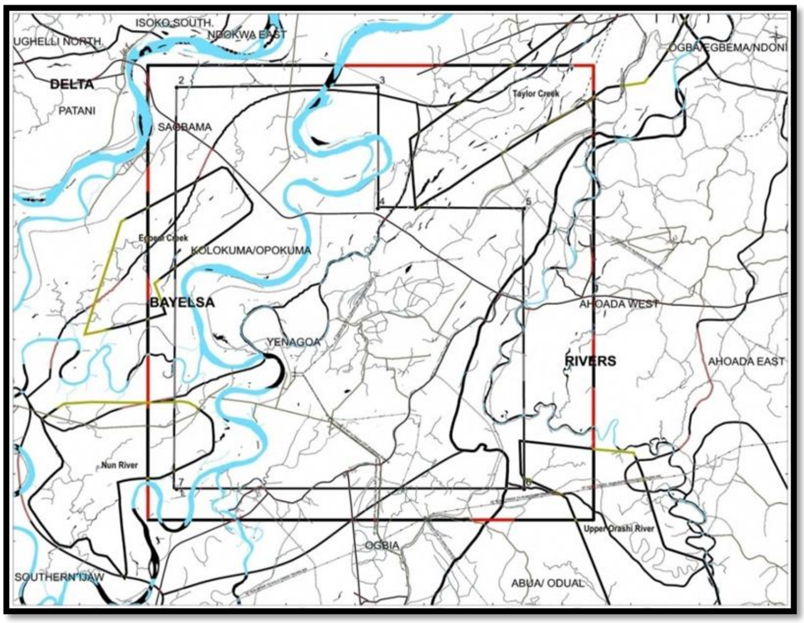

Figure 2: Location Map of study area (Gbaran field)

Methodology

The study's methodology involved the systematic partitioning of the prospect map into seven swaths to facilitate the acquisition process. The seismology department, overseeing seismic operations, collaborated with multiple divisions in the field, including the survey section, which aimed to establish seismic lines for drilling shot points. The creation of a base map and the designation of Global Positioning System (GPS) points by client codes were necessary for equipment calibration prior to line establishment in order to meet client specifications. Control lines were strategically devised to guide surveyors in connecting predetermined points for seismic line formation. Each of the seven swaths consists of twelve receiver lines. Shot points on source lines were marked with red or yellow ribbons, denoting source line number and receiver line number (X/Y), while receiver stations were marked with blue ribbons, denoting receiver line number and source line number (Y/X). The survey section submitted a comprehensive report to the seismology department post-line cutting. The field quality control unit, a subsidiary division, ensured precise line cutting, accurate peg assignment, and safe shot point establishment, adhering to regulatory safety standards. The drill section excavated single-deep holes (SDHs) using a semi-automated drilling system, burying dynamites for seismic energy. Drilling involved water pumps, swivel heads, drill stems, and drilling mud, reaching depths up to 70 meters. Two turners manipulated a T-shaped clamp during drilling, ensuring continuous mud flow for cutting removal. The recording section managed preloading, shooting, swath move, line check, LAUX crew, and recording platform operations. Preloading involved underground explosive placement using preloaders and a 55-metre lead detonator. Shooting operations employed a blaster to initiate explosive detonation, connecting wires to firing lines. Swath movers prioritised cable and geophone installation for signal acquisition. Field digitising units transformed analogue geophone data into digital format, while the LAUX crew established connections between receiver lines. Line checkers rectified errors using multimeters, assessing battery and cable voltages. The recording platform, which was attached to a land vehicle, recorded seismic reflections picked up by geophones. For workstation operations, Sercel equipment like the 408XL or 428XL Telemetry System was used. This comprehensive methodology ensured the effective execution of the 3D reshoot seismic survey in the Gbaran field of the Niger Delta.

Result and discussion

In this research, the GBARAN field preplot design was meticulously executed to ensure the guaranteed acquisition fold, thus avoiding fold drop. The source and receiver lines were successfully created in the designated field, emphasising environmental protection by relocating points originally situated on non-seismic objects or rivers. Strategic replanting and replacement of points were undertaken to ensure full-fold coverage of the impacted region and proper sampling of the subsurface. Figure 3 depicts four distinct approaches that were employed for relocating inaccessible shot points. These approaches include point shift, smooth curve, modified smooth curve, and laminar flow.

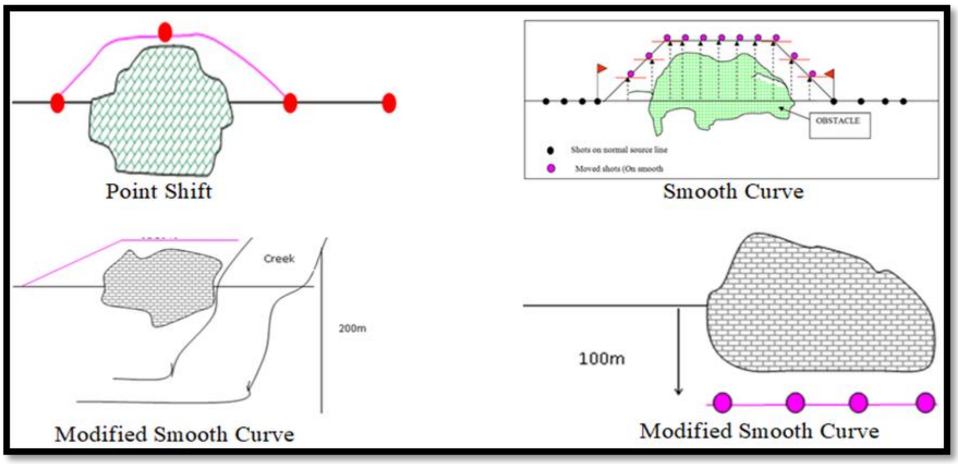

Figure 3: Different types of point offset.

These techniques allowed for safe positioning and contributed to the overall fold of the affected area. The entire OML 28 area was divided into seven swaths, and the fold coverage was computed for different offset ranges (near, mid, far, and full offset). The study revealed that the nominal full-fold coverage for the entire OML 28 area was 312.

These ranges are:

1. 0–3663 m (near offset range): Within this offset range, the fold coverage is between 76 and 90 folds, and it falls below the nominal full fold coverage.
2. 3663–7327 m (mid offset range): Within this offset range, the fold coverage was calculated to be 146–155 folds.
3. 7327–10990 m (far offset range): Within this offset range, the predominant coverage is 40–76 folds.

   0–10990 m (full offset): The nominal full-fold coverage is 312.

Figures 4 to 7 present a pictorial fold analysis of these offset ranges. The fold ranges were identified using the following hues in descending order: yellow, red, ash, green, turquoise blue, royal blue, and pink. The color bands are utilized for all the offset ranges that were sampled in this investigation.

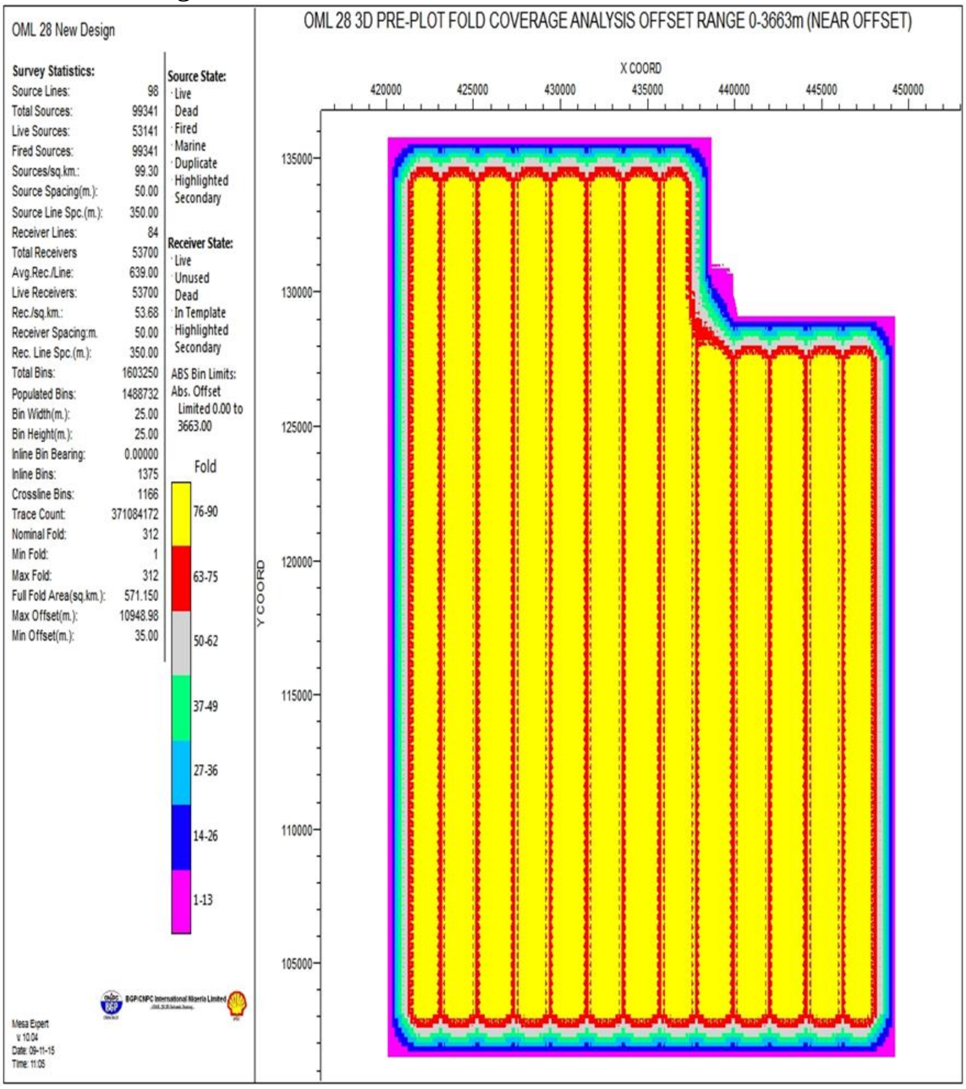

Figure 4: Pre-Plot coverage simulation of OML 28 3D (Near offset)

Figure 4 illustrates the frequency of acquisition events at near offset range, divided into seven distinct ranges. The near offset range (0–3663 m) refers to the starting side of the acquisition event, namely the side closest to the taper end of the field. Figure 4 indicates that the desired nominal fold of 312 was not attained due to the fact that only one side of the acquired field was utilized for sampling the subsurface. The near offset exhibits a fold range of 76 to 90, visually represented by the color yellow. The red hue represents the fold range of 63–75, appearing as parallel lines in the near offset area. The near offset range is delimited by the following fold ranges: 50–62, 37–49, 27–36, 14–26, and 1–13, which are represented by the colors ash, green, turquoise blue, royal blue, and pink, respectively. Due to insufficient sampling of the subsurface, the fold ranges provided do not allow for any conclusions to be drawn regarding the nature and potential of the subsurface.

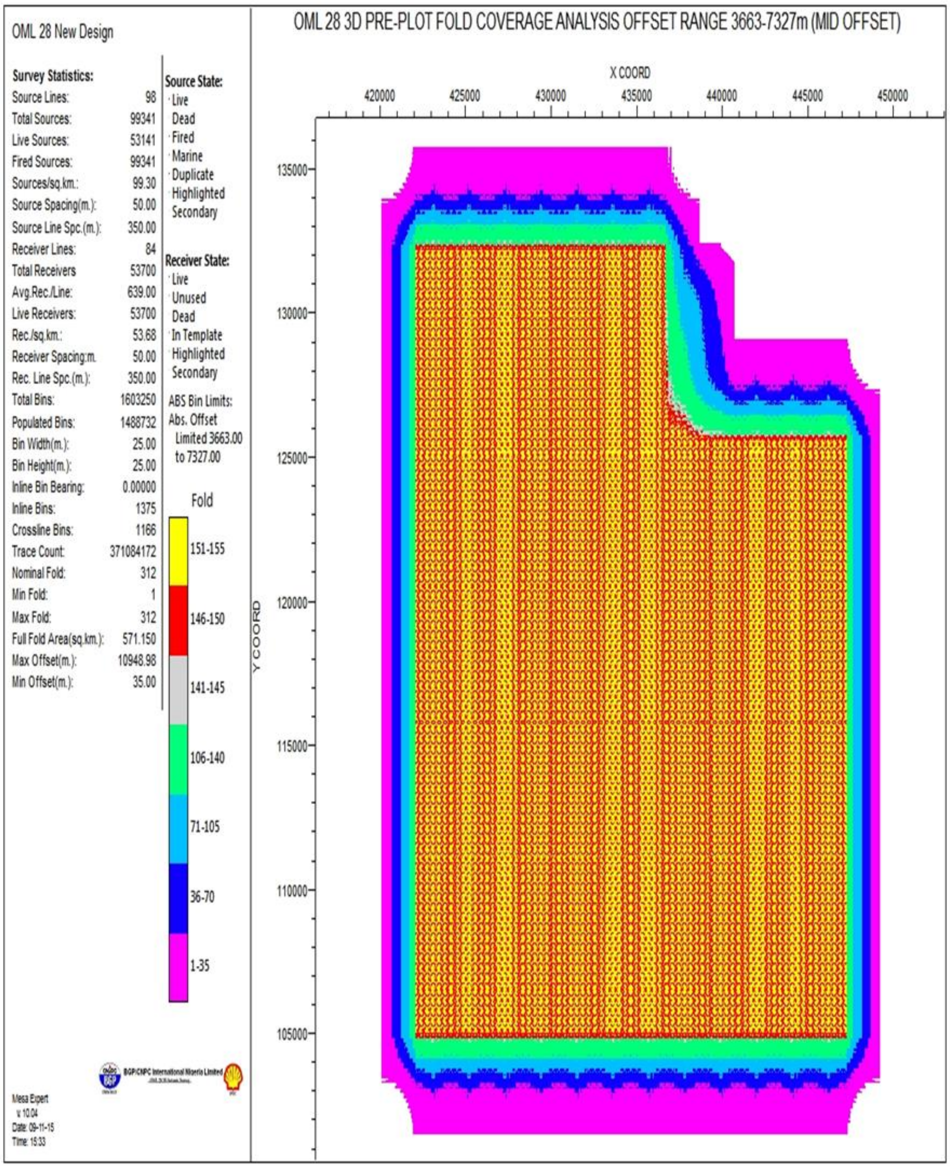

Figure 5: Pre-Plot coverage simulation of OML 28 3D (Mid offset)

Figure 5 displays the fold with a mid-offset range (3663–7327 meters). Compared to the near offset range fold in Figure 4, there is an increase in the acquisition fold in this case. The upper limit of the fold range in this context is between 151 and 155. These values are indicated by the color yellow. Next, there is a red fold shown, with range values of 146–150. The two ranges are observed to be intercalating with one another, as shown in Figure 5. The observed increase in the mid-offset range implies that shots outside of this range may be contributing to its fold, as a result of its position as the middle. Additional fold ranges discovered within the mid-offset range include of 141–145 (ash), 106–140 (green), 71–105 (turquoise blue), 36–70 (royal blue), and 1–35 (pink). Additionally, it was noted that the highest degree of fold in the near offset, represented by the first color band (yellow) in figure 4, aligns with the fifth color band (turquoise blue) in figure 5, which corresponds to the third lowest level of fold found in the mid offset range. This suggests that other shots outside the range under consideration have effect in building the mid offset range fold. Irrespective of how improved the fold in mid offset range is, it also failed to meet the nominal fold required.

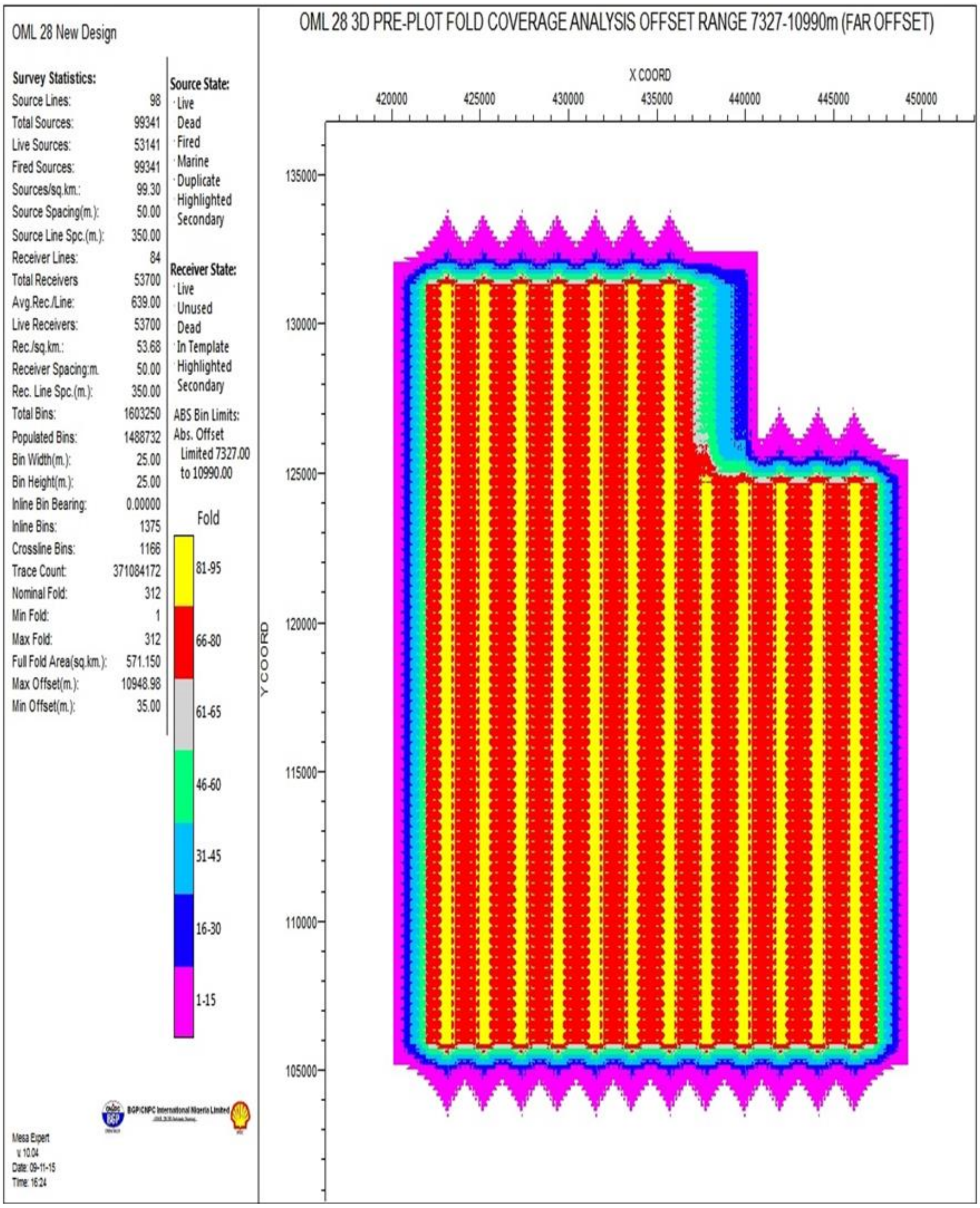

Figure 6: Pre-Plot coverage simulation of OML 28 3D (Far offset)

The far offset range (Figure 6) exhibited a fold trend that was comparable to the near offset range (Figure 4), indicating a similar pattern. This indicates that the far offset range is located at the other side of the taper end. The yellow band, representing the highest fold values, has a fold range of 81–95. Additional fold ranges that were noticed include 66–80 (red), 61–65 (ash), 46–60 (green), 31–45 (turquoise blue), 16–30 (royal blue), and 1–15 (pink). The far offset when compared to the mid offset, exhibited a similar pattern to what was observed when the near offset range was compared to the mid offset as well. The highest fold in the far offset, represented by the first color band (yellow) in figure 6, aligns with the fifth color band (turquoise blue) in the mid offset, as depicted in figure 5. This alignment corresponds to the third lowest fold observed within the mid offset range. This validates that shots taken from both the near and far offset ranges must have had a role in enhancing the fold observed within the mid offset range.

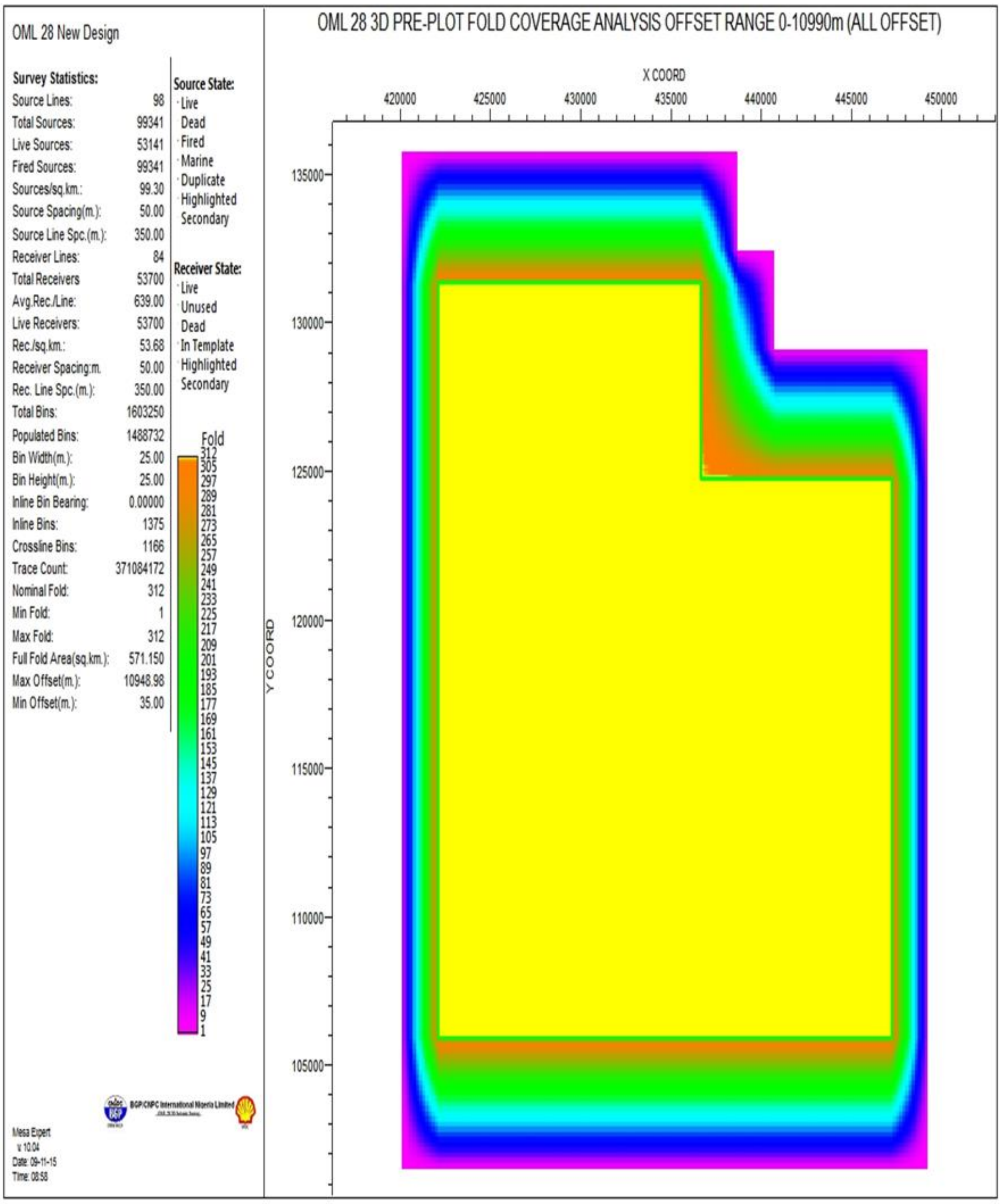

Figure 7: Pre-Plot coverage simulation of OML 28 3D (All offset)

Figure 7 represents the merging of all the offset ranges, including those that are near, middle, and far. The desired nominal fold was attained by merging the offset ranges. Although the boundaries of the field had some drops as compared to the nominal fold, but the resulting impact is quite insignificant. The region shown in yellow represents the specified nominal fold of 312. The nominal fold was attained due to the overlap of different ranges or swaths. This indicates that certain shots within a specific range or area can be acquired for another range in order to generate the required fold and accurately sample the subsurface within the target area. Overlap shots are not applicable to in all areas. Overlap shots are shots that are predominantly close to the area requiring fold enhancement. When planning the overlap shots, the receivers that receives the reflected energy are also taken into account. Figure 7 (all offset) provides a comprehensive sampling of the Gbaran field.

The distribution of offsets and azimuths was evaluated using bin statistics, offset/azimuth rose diagrams, and surface topography analysis. The bin data (Offset/Azimuth Rose Diagram) clearly indicate that a significant concentration of traces occurred between 140 and 220 degrees, as well as between 320 and 40 degrees. The offset plot displays a favorable and consistent distribution of offsets. Figures 8 and 9 illustrate the statistical data of the bins and the rose diagram that were produced as a result of the study.

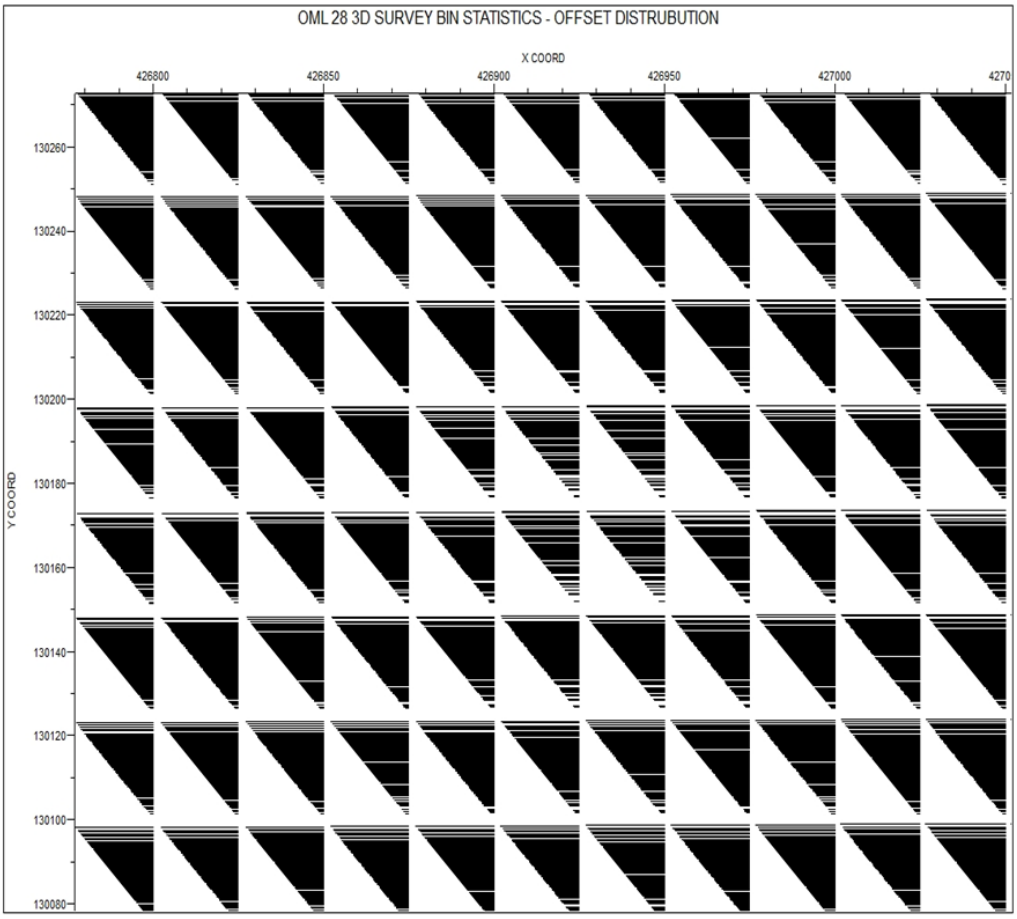

Figure 8: OML 28 offset distribution

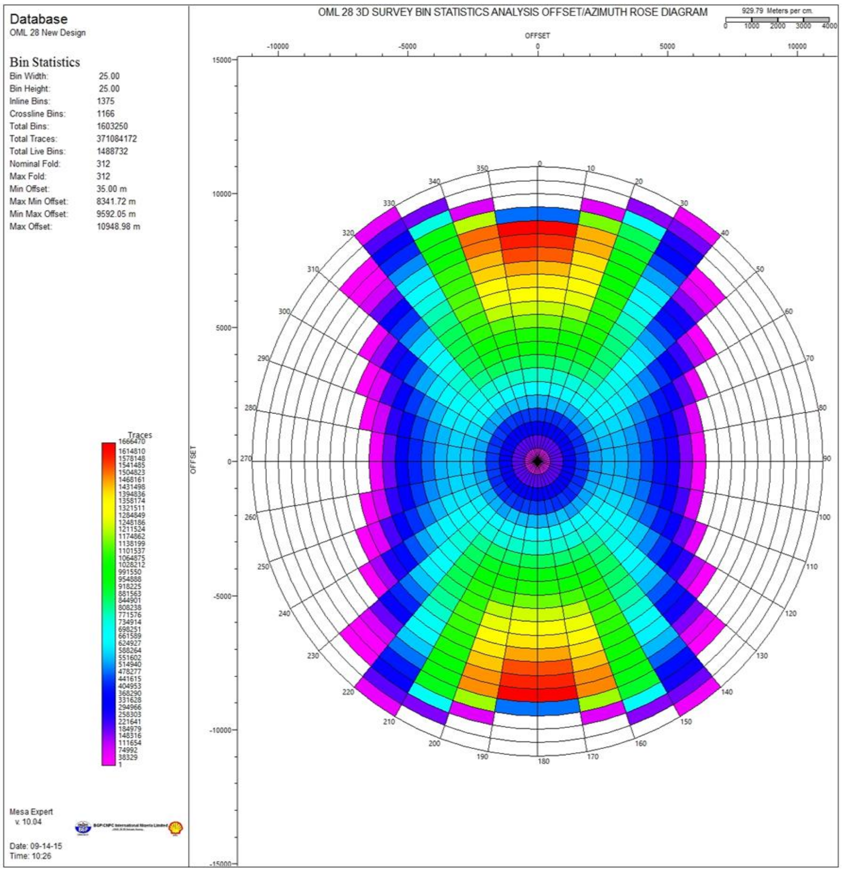

Figure 9: OML 28 Azimuth Distribution Plot

The topography analysis considered the natural features and elevation of the location, providing insights into the geological composition of the study area, with the highest elevation being 14.7 m. Figures 10 and 11 express the 3D and 2D models of the elevation of the study area.

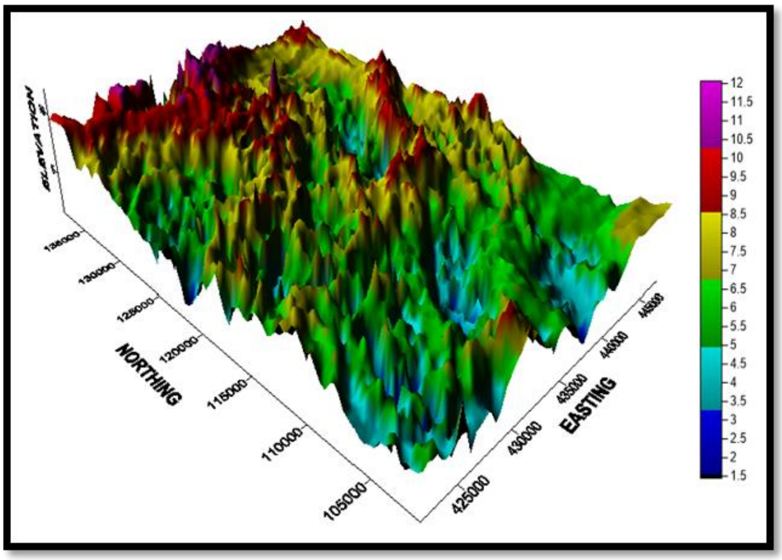

Figure 10: OML 28 3D Surface Expressions

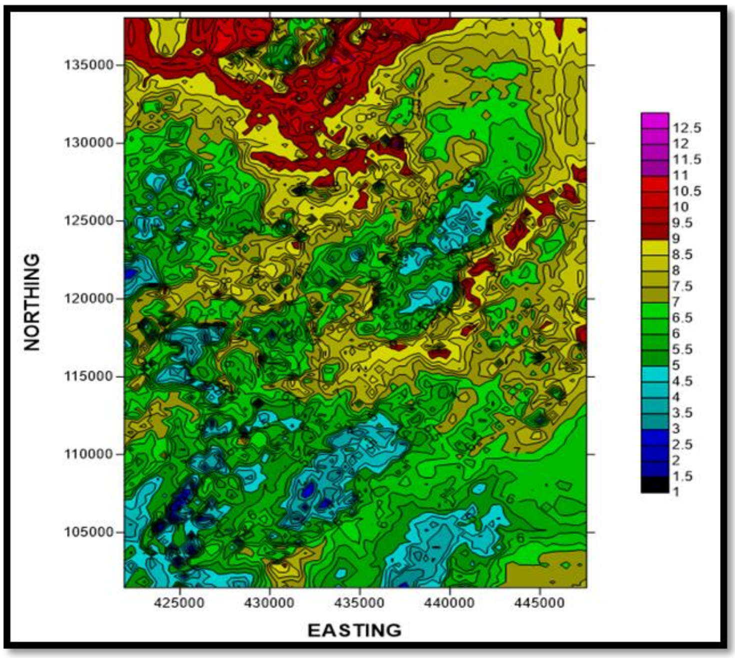

Figure 11: OML 28 2D topography map

Drilling operations were crucial for preparing shot points, and they involved the excavation of single-deep holes (SDHs) to a depth of 45 meters. However, the loading analysis revealed that all shot points were not loaded to full depth due to various factors like upthrust, back filling, etc., leading to a potential dampening effect on the signals produced. The loaded depth analysis illustrated that most shot points were loaded between 40 and 42m, with some reaching depths below 37m. The drilling and loaded gap analysis emphasised the discrepancy between the drilled depth and the depth at which shot points were loaded, highlighting the importance of addressing such disparities to avoid signal attenuation and ground roll issues. In this study, the smallest discrepancy between the drilled depth and loaded depth is 0.5m, while the largest discrepancy is 22.5m. The average difference between drilled depth and loaded depth stood at 4.6239m with respect to the GBARAN field. The results also indicated that the largest discrepancy between the depth at which drilling occurred and the depth at which loading took place corresponds to the minimum loaded depth of SDH, which is 22.5m. Figures 12, 13, and 14 indicate the 3D contour of loaded depth, the 3D expression of the gap between drilled depth and loaded depth, and the 2D expression of the gap between drilled depth and loaded depth, respectively.

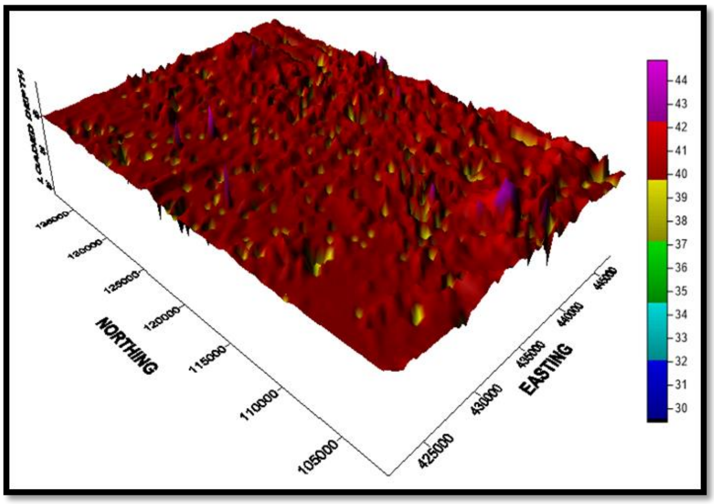

Figure 12: 3D contour of Loaded Depth

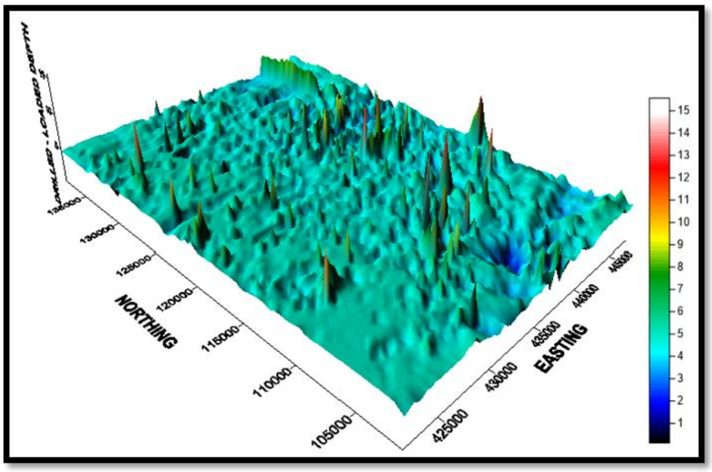

Figure 13: 3D expression of gap between drilled depth and loaded depth

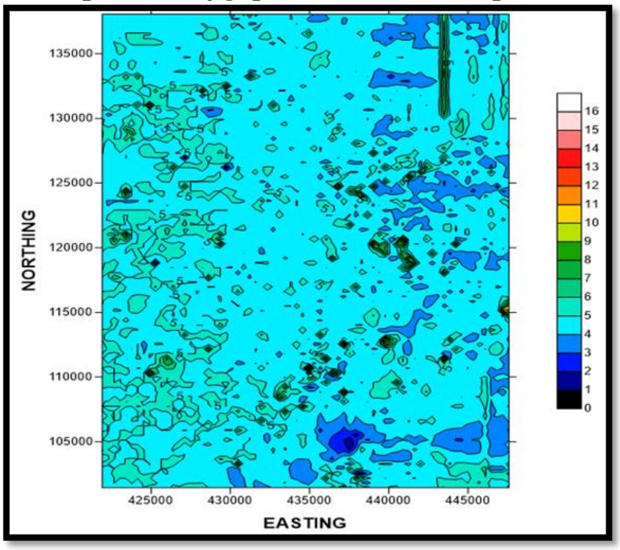

Figure 14: 2D expression of gap between drilled depth and loaded depth

Analysing the arrival time of 99,341 shot points acquired, covering an area of 7,615.45 square kilometres, it was also observed that it varied across different points due to the diverse composition of subsurface and varying distances between shots and receivers. Therefore, the importance of drilling past the weathered layers before burying energy sources to enhance signal velocity is of great importance to minimise the effect of signal attenuation in the weathered zone. The analysis indicated that the shortest arrival time recorded was 11 ms, while the longest was 99 ms, with an average arrival time of 25.70 ms for SDHs in the GBARAN field. Figures 15 to 17 illustrate a raw shot showing the arrival sequence of signals to receivers, a 2D plot of signal arrival time, and a 3D expression of signal arrival time.

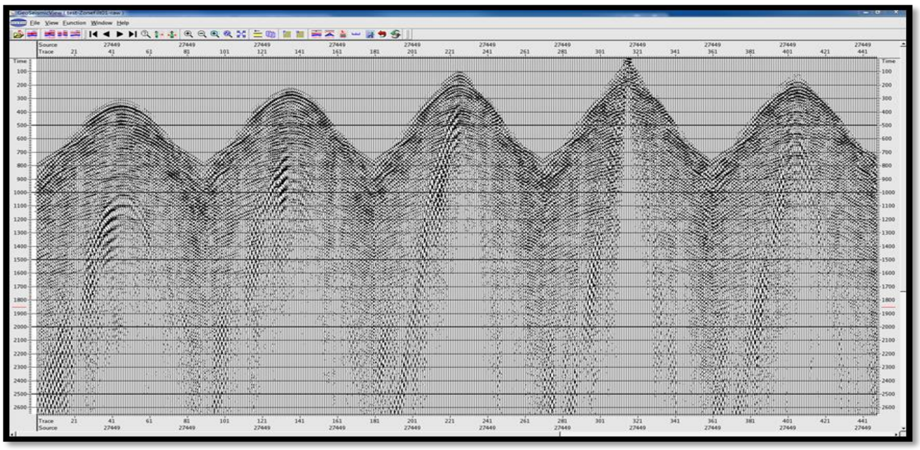

Figure 15: Raw shot showing arrival sequence of signals to receivers.

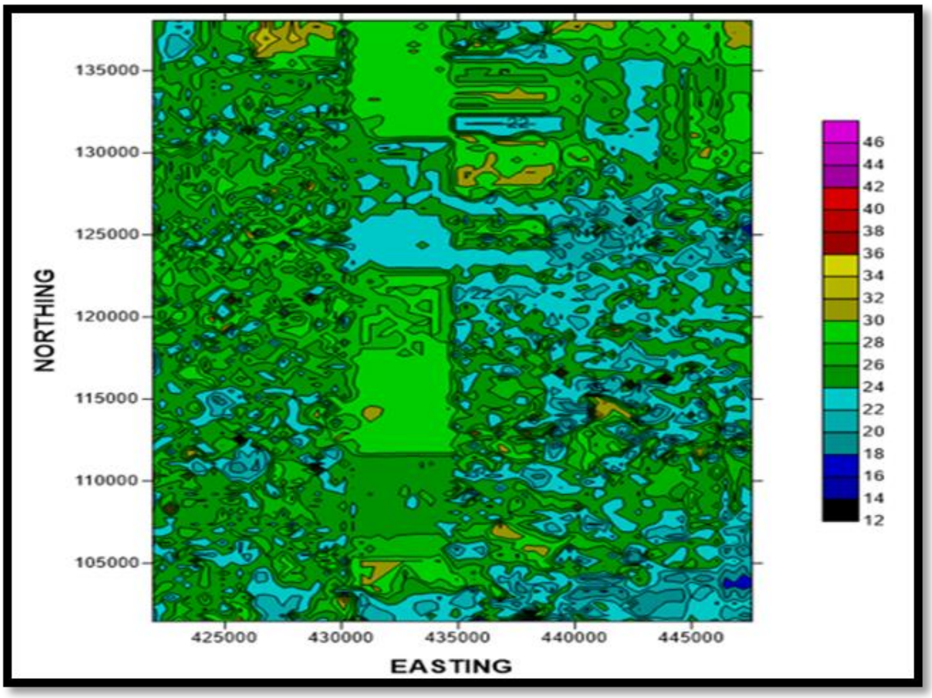

Figure 16: 2D plot of signal arrival time

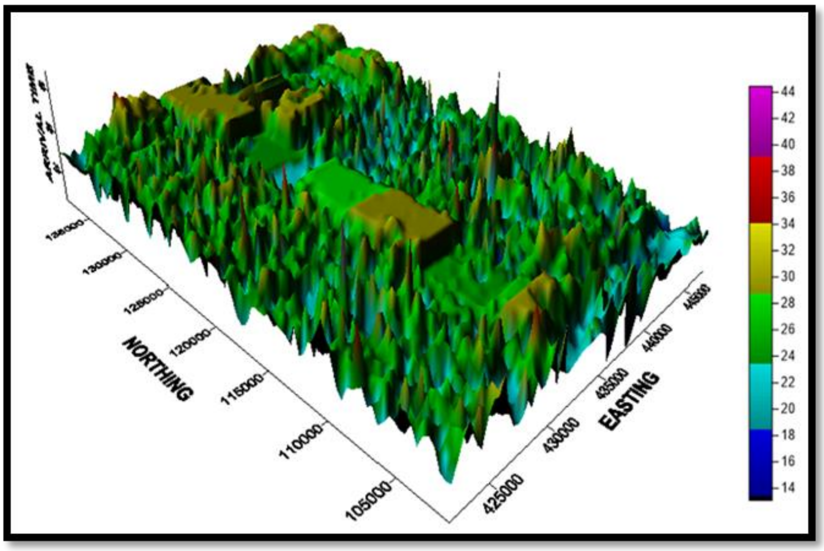

Figure 17: 3D expression of signal arrival time

Conclusion

In conclusion, this study has demonstrated the efficacy of seismic acquisition in delineating fold coverage analyses of the Niger Delta region, particularly exemplified in the OML 28 block case study. The seismic reflection method, despite facing challenges such as environmental variables and noise interference in densely populated urban areas, remains a vital tool for various applications including petroleum exploration, engineering site investigations, hydrogeological research, shallow stratigraphy, and archaeology.

The research methodology employed a systematic approach to partition the study area into seven swaths, ensuring effective acquisition of seismic data. Through meticulous execution of the preplot design and strategic relocation of shot points, the study aimed to achieve optimal fold coverage across different offset ranges. Analysis of fold coverage revealed varying ranges across different offset intervals: Near offset range (0–3663 m) exhibited a maximum foldcoverage range of 76 and 90, falling below the nominal full-fold coverage of 312; Mid offset range (3663–7327 m) demonstrated improved maximum fold coverage, ranging from 151 to 155 folds. Far offset range (7327–10990 m) predominantly showed maximum fold coverage between 81 and 95 folds. Full offset range (0–10990 m) achieved the nominal full-fold coverage of 312.

Integration of various techniques including point shift, smooth curve, modified smooth curve, and laminar flow for relocating inaccessible shot points contributed to achieving the desired fold coverage. Moreover, the study employed bin statistics, offset/azimuth rose diagrams, and surface topography analysis to assess the distribution of offsets and azimuths, providing valuable insights into the geological composition of the study area.

Drilling operations played a crucial role in preparing shot points, with analysis revealing discrepancies between drilled depth and loaded depth, emphasizing the need for addressing such disparities to avoid signal attenuation issues. Furthermore, analysis of arrival time variation across different shot points underscored the importance of drilling past weathered layers to enhance signal velocity and minimize signal attenuation in the weathered zone.

Overall, this study highlights the significance of seismic acquisition methodologies in characterizing subsurface structures and geological features, providing valuable insights for various applications in the exploration and understanding of the Earth's subsurface dynamics.

Recommendations

- **Optimize Shot Point Relocation**: Further optimization of shot point relocation techniques, such as point shift, smooth curve, modified smooth curve, and laminar flow, should be explored to ensure comprehensive coverage and sampling of the subsurface. Additionally, continuous monitoring and adjustment of shot point positions during seismic acquisition can help improve fold coverage, especially in challenging terrains like the Niger Delta.
- **Enhance Environmental Protection Measures**: Strengthening environmental protection measures during seismic acquisition is imperative. Efforts should focus on minimizing disturbances to non-seismic objects and water bodies, including rivers, through strategic replanting and replacement of shot points. Comprehensive environmental impact assessments should be conducted prior to survey operations to identify and mitigate potential ecological risks.
- **Improve Swath Overlap Planning**: Enhancing planning strategies for swath overlap can aid in achieving the desired nominal fold coverage. Incorporating overlap shots strategically, particularly in areas with lower fold coverage, can help ensure thorough subsurface sampling and improve imaging resolution. Careful consideration of receiver placements and shot point distributions is essential for effective swath overlap implementation.
- **Address Drilling Depth Discrepancies**: Efforts should be made to address discrepancies between drilled depth and loaded depth during shot point preparation. Implementing measures to minimize factors contributing to depth variations, such as upthrust and backfilling, is crucial for optimizing signal transmission and reducing signal attenuation issues. Continuous monitoring and quality control measures throughout drilling operations are essential to ensure accurate depth loading.
- **Enhance Signal Velocity in Weathered Zones**: Given the variation in signal arrival times across different subsurface compositions and distances between shots and receivers, drilling past weathered layers before burying energy sources should be prioritized. This practice can enhance signal velocity and minimize signal attenuation effects in weathered zones, thereby improving subsurface imaging quality and interpretation accuracy.

Overall, these recommendations aim to optimize seismic acquisition operations, mitigate environmental impacts, and enhance subsurface imaging capabilities in complex terrains like the Niger Delta, ultimately facilitating improved geological understanding and resource exploration. Continued research and technological advancements in seismic acquisition methodologies are essential for addressing existing challenges and maximizing exploration potential.

Acknowledgement

My profound gratitude goes to Bureau of geophysical Prospecting Nigeria Limited (Crew 8619), a subsidiary of china National Petroleum Cooperation (CNPC) for making their platform available for this research.

Author Contribution

Onwubuariri, Chukwuebuka Nnamdi conceptualized and designed the research under the supervision of Anakwuba, Emmanuel Kenechukwu. Dinneya, Obinna Christian and Nwokoma, EsomchiUzoma reviewed existing literature and data. Onwubuariri, Chukwuebuka Nnamdi, interpreted the result under the supervision of Anakwuba Emmanuel Kenechukwu. All the authors contributed to writing the research draft, read and approved the final manuscript.

Data Availability

The data set used will be made available on request from the corresponding author.

Ethics Approval

The paper reflects the authors' research and analysis in its complete and truthful manner

Conflicts of Interest

There is none to declare

References

Adizua, O.F., Anakwuba, K.E., Onwuemesi, A.G. (2019). Derivation of refraction statics solution for 3D seismic data in an onshore prospect Niger Delta field. Geology, Geophysics & Environment.

Ajani, O. O., Fajemiroye, J. A., & Odumosu, O. A. (2013). Study of Near-surface Layer of Omerelu area using Low Velocity Layer (LVL) Method. International Journal of Development and Sustainability, 2(1), 131-139.

Anomoharan O (2014) Downhole seismic refraction survey Of weathered layer characteristics in Escravos Nigeria. Am J ApplSci 11(3): 371–380.

Bridle, R., & Aramco, S. (2009). Delay-Time Refraction Methods applied to a 3D Seismic Block. The Leading Edge Publication, 28(2), 228–237

Cordsen, A., Galbraith, M., & Peirce, J. (2000).Planning Land 3-D Seismic Surveys. Geophysical Developments Series No. 9.Society of Exploration Geophysicists. Corsmit, J., Versteeg, W.

Doust H, Omatsola E (1990) Niger delta. In: Edwards JD, Santogrossi PA (eds) Divergent/passive margin basins AAPG Memoir 48. American Association of Petroleum Geologists

Ejedawe JE (1981) Patterns of incidence of oil reserves in Niger Delta Basin. American Association of Petroleum Geologists (AAPG), vol. 65.

Hewitt, J. (1980). Seismic Data Acquisition. SEG Continuing Educational Program, Soc. Exploration Geophysics, Tulsa.

Kolawole, F., Okoro, C., & Olaleye, P. (2012). Downhole refraction survey in the Niger Delta Basin: A 3-layer model. ARPN Journal of Earth Sciences, 1(2).

Opara, C., Adizua, O. F., & Ebeniro, J. O. (2018). Application of static correction in the processing of 3D seismic data from onshore Niger Delta. Universal Journal of Geoscience UJG, 6(1), 1-7.

Opara, C., Adizua, O. F., & Ebeniro, J. O. (2017). Near-surface seismic velocity model building from first arrival travel-times – A case study from onshore, Niger – Delta. Universal Journal of Physics and Application UJPA, 12(1), 1-10.

Onwubuariri, C. N., Anakwuba, E. K., Nwokoma, E. U., Dinneya, O. C., & Osaki, L. J. (2023). Implications of Fold Monitoring in Seismic Data Acquisition: Case Study of Niger Delta. Nigerian Journal of Physics (NJP), Volume 32(2), ISSN: 1595-0611, pp 1 – 22.

Onwubuariri, C. N., Nnanna, L. A., Anakwuba, E. K., Mgbeojedo, T. I., Agoha, C. C., Nwaeju, C. C., Osaki, L. J., &Nwaneho, F. U. (2022). Environmental and geophysical Implications of drilling Techniques employed in onshore Seismic data acquisition. International Journal of Engineering Applied Sciences and Technology, 7(6), ISSN No. 2455-2143, Pages 101-116.

Yordkayhun, S., Juhlin, C., Giese, R., &Cosma, C. (2007). Shallow Velocity–Depth Model using first arrival travel-time inversion at the CO2SINK site, Ketzin, Germany. Journal of Applied Geophysics, 63, 68-79.

Zanzi, L., &Carlini, A. (1991).Refraction statics in the wavenumber domain. Geophysics, 56, 1661- 1670.